Quantum Dynamics of the Vibrations of Helium Bound to the Nanosurface of a Large Planar Organic Molecule: Phthalocyanine·He van der Waals Complex†

Brittney R. Gibbons, Minzhong Xu, and Zlatko Bačić*

Department of Chemistry, New York University, New York, New York 10003

Received: October 23, 2008; Revised Manuscript Received: December 5, 2008

We report rigorous quantum three-dimensional calculations of highly excited intermolecular vibrational states of the van der Waals (vdW) complex phthalocyanine·He (Pc·He). The Pc molecule was treated as rigid and the intermolecular potential energy surface (IPES) was represented as a sum of atom−atom Lennard-Jones pair potentials. The IPES has four equivalent global minima on the diagonals of the square-shaped Pc, inside its five-membered rings, and four slightly shallower local minima between them, creating a distinctive corrugation pattern of the molecular nanosurface. The vdW vibrational states analyzed in this work extend to about two-thirds of the well depth of the IPES. For the assignment of the in-plane (*xy*) vdW vibrational excitations it was necessary to resort to two sets of quantum numbers, the Cartesian quantum numbers [v_x, v_y] and the quantum numbers (v, l) of the 2D isotropic oscillator, depending on the nodal structure and the symmetry of the wave functions. The delocalization of the He atom parallel to the molecular surface is large already in the ground vdW state. It increases rapidly with the number of quanta in the in-plane vdW vibrations, with the maximum root-mean-square amplitudes Δx and Δy of about 7 au at the excitation energies around 40 cm^{-1}. The wave functions of the highly excited states tend to be delocalized over the entire nanosurface and often have a square shape, reflecting that of the substrate.

I. Introduction

Liquid helium droplets provide an ultracold and gentle, uniquely homogeneous quantum matrix for high-resolution molecular spectroscopy.[1−3] Recent years have witnessed considerable activity in the area of the electronic spectroscopy of large planar organic molecules in helium droplets.[3−14] These molecules can be viewed as nanoscale precursors to a bulk graphite surface, with the added advantage that both the shape and the size of the substrate, as well as the nature of the surface corrugation, can be varied systematically. Thus, linear polyacenes from benzene to tetra- and pentacene, with one to five aromatic rings, provide model quasi-one-dimensional (1D) nanosurfaces of gradually increasing length, while porphin and phthalocyanine constitute quasi-2D, nearly square-shaped nanosubstrates for helium adsorption.

Experimental studies involving the electronic spectroscopy of helium-solvated large aromatic molecules fall in two broad classes: (i) those where the number of He atoms n is small ($n = 1-16$) and (ii) those with an aromatic molecule embedded in a helium nanodroplet ($n = 10^3-10^4$). In the two-color resonant two-photon ionization spectra of the electronic $S_1 \leftarrow S_0$ transition of the 2,3-dimethylnaphthalene·He (2,3-DMN·He) van der Waals (vdW) complex,[15] five bands were observed within 30 cm^{-1} of the electronic origin. On the basis of the quantum 3D bound-state calculations, four bands were assigned to intermolecular vibrational excitations in the S_1 excited electronic state, and the fifth to a vdW isomer.[15] For a small number of He atoms bound to naphthalene,[16] anthracene,[16,17] and tetracene,[16] the vibronic spectra of the $S_1 \leftarrow S_0$ transition exhibit discrete bands on the high-frequency side of the 0_0^0 transition, corresponding to the vdW vibrations in the S_1 state. The number of vibronic bands reaches a maximum of six, for tetracene solvated with 4 and 5 He atoms, and then surprisingly diminishes rapidly for larger clusters. By $n = 7$, only a single vibronic band remains, 20 cm^{-1} to the blue of the origin.[16] It has been suggested that this peculiar size evolution of the vibronic structure reflects the change of the character of the helium vibrations, from localized modes to collective excitations.[3]

Inside helium droplets, in the excitation spectra of the $S_1 \leftarrow S_0$ transition of large aromatic molecules the 0_0^0 origin and each vibronic band display a sharp zero-phonon line (ZPL), a pure molecular transition shifted by 10−100 cm^{-1} to the red or blue from the corresponding gas-phase frequency due to the interaction with the helium solvent, followed by a weaker phonon wing (PW) on the high-frequency side.[3] The PWs are thought to arise from the collective compressional excitations of the helium cluster coupled to the electronic excitation of the dopant molecule.[3,6] The ZPLs of some molecules in helium are split; one example is the ZPL of the 0_0^0 band of tetracene, which appears as a pair of sharp lines 1.1 cm^{-1} apart.[4−6] This splitting of the ZPL is not observed in small helium clusters,[16] and its origin is not well understood at this time, despite intense scrutiny and various models put forth to explain it.[6]

Phthalocyanine (Pc), with the molecular formula $C_{32}N_8H_{18}$ and D_{2h} symmetry, is one of the largest organic molecules whose vibronic spectrum in helium droplets has been investigated. The absorption spectrum of its $S_1 \leftarrow S_0$ transition exhibits the single ZPL of the 0_0^0 band, accompanied by the PW which is 3−5 cm^{-1} to the blue of the ZPL.[3,6,11] The ZPL is red-shifted by 43 cm^{-1} from that of the free molecule, as a result of the difference between the Pc−He interactions in the S_0 and S_1 electronic states of Pc. The high-resolution spectrum of the PW shows rather sharp, discrete features at 3.0, 3.8, and 5.0 cm^{-1} from the ZPL. These features may correspond to the collective vibrational excitations of the first helium shell around the Pc molecule.[3,11]

† Part of the "George C. Schatz Festschrift".

* Author to whom correspondence should be addressed. E-mail: zlatko.bacic@nyu.edu.

10.1021/jp809410s CCC: $40.75
Published on Web 01/14/2009

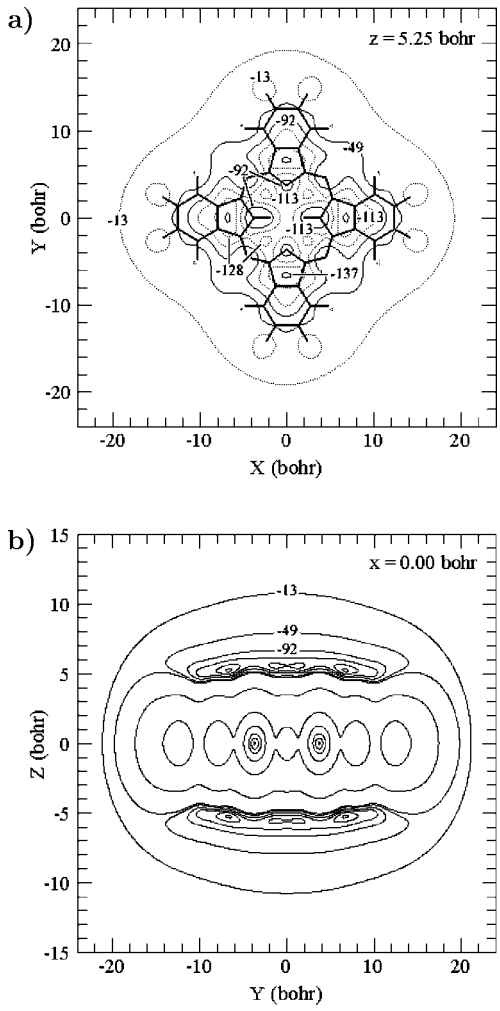

Figure 1. Contour plots of the intermolecular potential energy surface (IPES) of phthalocyanine·He for the parameters in Table 1. Shown are the potential cuts in (a) the *xy* plane for $z = 5.25$ au, the z coordinate of the global minimum of the IPES, and (b) the *yz* plane for $x = 0.0$ au.

TABLE 1: Lennard-Jones Atom−Atom Potential Parameters σ and ε for Phthalocyanine·He Used in This Work (from ref 19)

interaction	σ (au)	ε (cm^{-1})
He−C	5.18	11.33
He−H	6.07	4.17
He−N	5.61	20.02

Due to strong vdW interaction of Pc and helium, the first layer of He atoms on both surfaces of Pc, more tightly bound and more localized than the subsequent helium solvent shells, could have its own excitation spectrum, distinct from the collective excitations of the bulk liquid helium.[11]

However, the helium layer surrounding Pc or any other large aromatic molecule represents a fluxional quantum many-body system of high dimensionality, and accurate calculation of the spectrum of its vibrational excitations is presently not feasible. This precludes, for the time being, the quantitative investigations of the above features observed in the PWs of Pc in helium droplets. The energetics and the structural properties of the solvation of Pc by helium have been studied with quantum Monte Carlo methods for He_n ($n \leq 24$) clusters in the ground state,[18] and at very low temperatures ($T = 0.625$ K) for n ranging from 24 to 150.[19]

TABLE 2: Properties of the van der Waals Vibrational Levels of Phthalocyanine·He in the S_0 State Calculated by Using the 3D DVR Method[a]

ΔE	Δx	Δy	Δz	$\langle z \rangle$	symmetry	$[v_x, v_y, v_z]$ or $(v, \lvert l \rvert, v_z)$
0.000	2.11	2.87	0.54	5.95	A_g, B_{1u}	(0, 0, 0)
1.718	1.69	4.94	0.55	5.86	B_{3g}, B_{2u}	[0, 1, 0]
2.627	5.93	1.62	0.55	5.80	B_{2g}, B_{3u}	[1, 0, 0]
3.055	5.41	3.85	0.54	5.74	A_g, B_{1u}	(2, 2, 0)
3.573	3.75	4.89	0.55	5.75	A_g, B_{1u}	(2, 0, 0)
4.974	1.79	5.27	0.55	5.80	B_{3g}, B_{2u}	[0, 3, 0]
5.648	4.26	2.54	0.55	5.88	B_{2g}, B_{3u}	[3, 0, 0]
6.193	2.95	3.17	0.54	5.94	B_{1g}, A_u	(2, 2, 0)
10.173	3.13	3.54	0.56	5.90	A_g, B_{1u}	(4, 0, 0)
11.641	5.33	2.50	0.55	5.86	B_{3g}, B_{2u}	(3, 1, 0)
12.424	3.08	5.20	0.56	5.85	B_{2g}, B_{3u}	(3, 1, 0)
12.455	4.35	3.93	0.58	5.90	A_g, B_{1u}	(4, 2, 0)
12.522	5.11	3.93	0.55	5.80	B_{1g}, A_u	(4, 4, 0)
14.305	3.98	5.06	0.55	5.77	B_{1g}, A_u	(4, 2, 0)
15.144	1.46	6.11	0.57	5.82	B_{3g}, B_{2u}	[0, 5, 0]
15.489	6.13	2.59	0.57	5.81	B_{2g}, B_{3u}	[5, 0, 0]
16.911	4.88	3.09	0.56	5.85	B_{3g}, B_{2u}	[4, 1, 0]
17.818	5.25	4.86	0.56	5.76	A_g, B_{1u}	
18.571	2.92	4.40	0.57	5.93	B_{2g}, B_{3u}	[1, 4, 0]
20.067	4.29	5.31	0.58	5.81	A_g, B_{1u}	
21.625	4.67	3.68	0.58	5.91	A_g, B_{1u}	
22.432	5.05	3.55	0.57	5.85	B_{1g}, A_u	[5, 1, 0]
22.490	6.50	2.75	0.57	5.80	B_{2g}, B_{3u}	
22.840	2.74	6.57	0.57	5.78	B_{3g}, B_{2u}	
23.825	3.04	4.81	0.57	5.90	B_{1g}, A_u	[1, 5, 0]
24.043	5.12	4.68	0.56	5.81	A_g, B_{1u}	
24.182	2.60	6.21	0.57	5.83	B_{3g}, B_{2u}	
24.368	6.34	2.50	0.58	5.82	B_{2g}, B_{3u}	
27.159	5.31	5.19	0.59	5.78	A_g, B_{1u}	
27.859	5.68	3.49	0.57	5.83	B_{3g}, B_{2u}	[6, 1, 0]
28.248	2.99	5.99	0.57	5.81	A_g, B_{1u}	
28.588	3.61	5.59	0.58	5.84	B_{2g}, B_{3u}	[1, 6, 0]
29.087	5.64	3.46	0.60	5.86	A_g, B_{1u}	
30.651	5.03	4.63	0.57	5.90	B_{1g}, A_u	
31.017	5.10	4.20	0.59	5.91	B_{2g}, B_{3u}	
31.244	4.56	4.77	0.59	5.92	B_{3g}, B_{2u}	
33.233	2.29	6.92	0.58	5.80	B_{3g}, B_{2u}	
33.340	6.36	2.92	0.57	5.85	B_{1g}, A_u	[7, 1, 0]
33.646	6.39	3.35	0.59	5.84	B_{2g}, B_{3u}	
34.201	2.83	6.45	0.57	5.85	B_{1g}, A_u	[1, 7, 0]
35.240	5.13	4.55	0.58	5.87	B_{3g}, B_{2u}	
35.677	5.16	5.20	0.57	5.82	B_{1g}, A_u	
35.724	5.64	4.40	0.58	5.84	A_g, B_{1u}	
35.724	4.80	4.80	0.59	5.89	B_{2g}, B_{3u}	
37.355	4.52	5.48	0.64	5.94	A_g, B_{1u}	
37.905	6.84	2.76	0.59	5.83	B_{3g}, B_{2u}	[8, 1, 0]
38.571	4.05	6.15	0.60	5.84	A_g, B_{1u}	
38.731	2.56	6.93	0.59	5.85	B_{2g}, B_{3u}	[1, 8, 0]

[a] The excitation energies ΔE (in cm^{-1}) are relative to the ground-state energy $E_0 = -92.268$ cm^{-1}. $\langle z \rangle$ and the root-mean-square amplitudes Δx, Δy, and Δz are in au. The levels are labeled by the irreducible representations of the D_{2h} symmetry group. The assignments are in terms of either the Cartesian quantum numbers $[v_x, v_y, v_z]$ or $(v, \lvert l \rvert, v_z)$, where v and l are the quantum numbers of the 2D isotropic oscillator defined in the text.

Even for the case of a single He atom bound to the surface of a large aromatic molecule, our understanding of the quantum dynamics of its excited intermolecular vibrations, and how it is related to the geometry of the substrate and its corrugation, is limited. Recently, we reported quantum 3D calculations of highly excited intermolecular vibrational states of the vdW complexes tetracene·He and pentacene·He in the S_1 state[20] (paper I). This study provided detailed information about the vdW vibrational level structure, mode coupling, and extensive wave function delocalization on large aromatic surfaces corrugated in the direction of

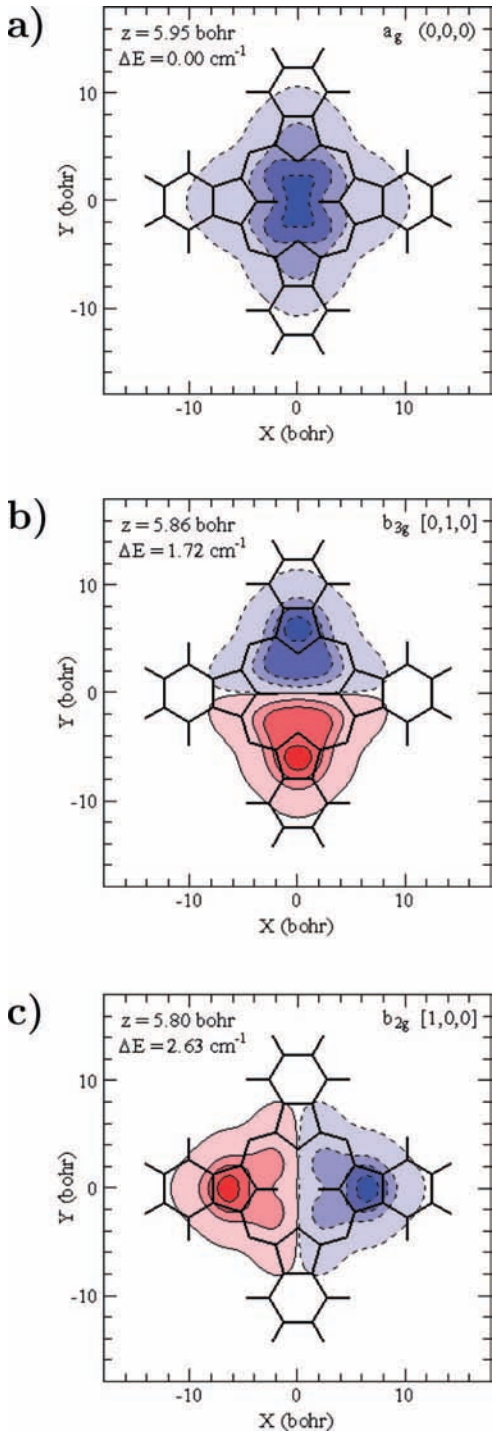

Figure 2. Cuts in the *xy* plane through the wave functions of the vdW vibrational ground state (a) and the two vdW vibrational states with one quantum in the in-plane *y* and *x* modes (b, c) at *z* corresponding to the expectation value $\langle z \rangle$ for each state. Contours are for 80%, 50%, 25%, and 1% of the maximum amplitude for the respective cuts.

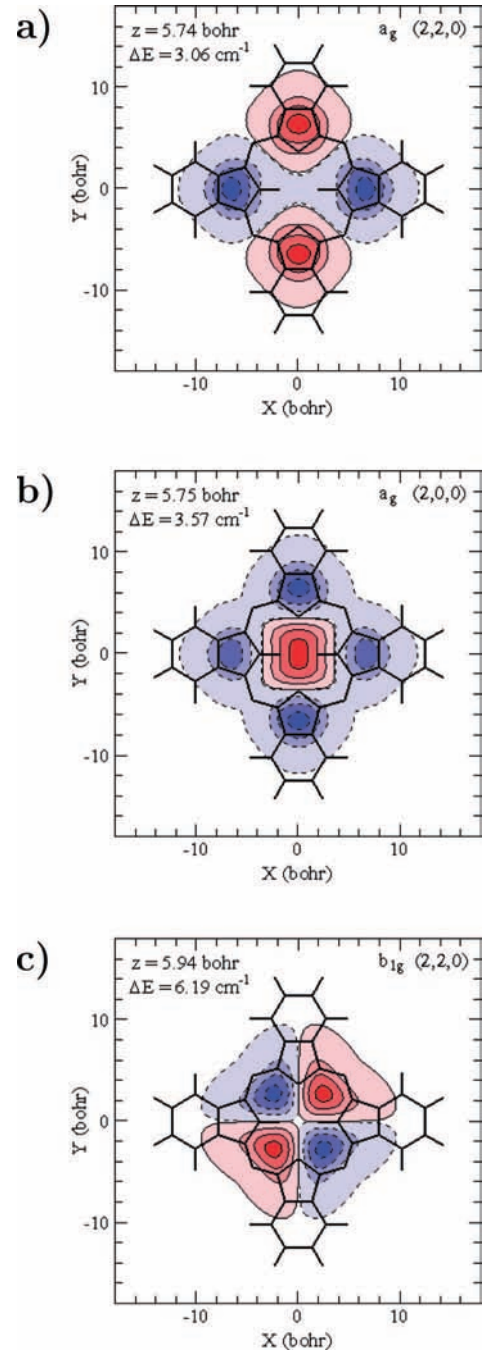

Figure 3. Cuts in the *xy* plane through the wave functions of the three vdW vibrational states with two quanta in the in-plane modes at *z* corresponding to the expectation value $\langle z \rangle$ for each state. Contours are for 80%, 50%, 25%, and 1% of the maximum amplitude for the respective cuts.

the long molecular axis. Bound-state calculations for helium on anthracene have also been published.[21−23]

The Pc molecule offers a planar nanosurface for helium adsorption that differs greatly from those of tetra- and pentacene in terms of shape, size, and corrugation. Tetra- and pentacene, having four and five benzene rings arranged linearly, are close to rectangular, with one in-plane molecular axis (*x*) substantially longer than the other (*y*). Their shape is mirrored in the intermolecular potential energy surfaces (IPESs) for tetracene·He and pentacene·He vdW complexes. Cuts through the IPES parallel to the molecular surface, for the out-of-plane (*z*) coordinate set to that of the global minimum, form nearly rectangular 2D potential basins with distinctly unequal neighboring sides, as shown by the potential energy contours in Figure 1 of ref 20. The basins are shallow, with the well depth of about -100 cm^{-1}, and exhibit weak corrugation of $10-13$ cm^{-1} along the long axis of the aromatic substrate. These features of the IPESs give rise to the in-plane vdW vibrational excitations in the *x* and *y* directions which have very different fundamental frequencies, are weakly coupled, and can be readily assigned in terms of the Cartesian quantum numbers.[20]

In contrast, the Pc molecule has essentially a square shape, which is also the shape of the 2D He-Pc vdW potential basin

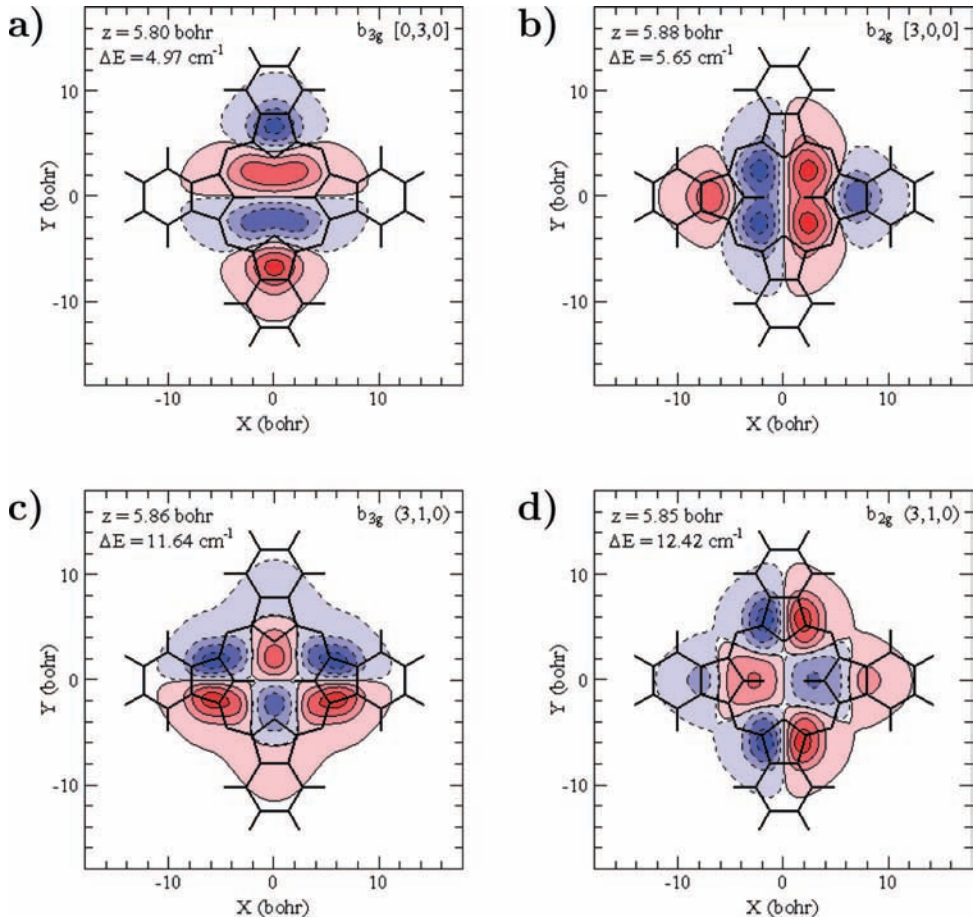

Figure 4. Cuts in the *xy* plane through the wave functions of the four vdW vibrational states with three quanta in the in-plane modes at *z* corresponding to the expectation value $\langle z \rangle$ for each state. Contours are for 80%, 50%, 25%, and 1% of the maximum amplitude for the respective cuts.

parallel to the surface of the molecule. As shown in Figure 1, the contour drawn at energy -92 cm^{-1}, which is the vdW vibrational ground-state energy of Pc·He, and for the *z* coordinate of the global minimum, defines the square potential basin with the side about 16 au long. By coincidence, the dimension of its diagonal, ~23 au, is very close to the length of the rectangular 2D potential basin for pentacene·He at the vdW zero-point energy (ZPE) of the complex (~40 cm^{-1}), whose width is about 10 au; see Figure 1 of ref 20. Due to the square-shaped 2D potential basin trapping the He atom, the energy level structure and the quantum number assignment of the in-plane vdW vibrational excitations of Pc·He are qualitatively different from those of tetracene·He and pentacene·He.

In this paper, we present the results of accurate quantum 3D calculations of highly excited intermolecular vibrational energy levels and wave functions of the Pc·He vdW complex in the ground electronic state S_0. Converged eigenstates reported and analyzed here extend up to ~45 cm^{-1} above the vdW vibrational ground state, covering about two-thirds of the well depth of the IPES employed. They provide for the first time a quantitative description of the complex vibrational dynamics of the He atom physisorbed on an intricately corrugated, square-shaped surface of a very large aromatic molecule.

II. Theory and Computational Aspects

A. Quantum 3D Calculations of the Intermolecular Vibrational Energy Levels. The methodology used in this work to compute the 3D intermolecular vibrational ($J = 0$) levels of Pc·He was developed by Mandziuk and Bačić[24] and applied to a variety of vdW M·R complexes,[15,25−28] including tetracene·He and pentacene·He in paper I.[20] A detailed description of the methodology is available,[24] so that only a brief summary is provided here.

The large molecule M, in this case Pc, is assumed to be rigid while the 3D subspace of the vdW vibrations of the complex is treated rigorously, as fully coupled. Treating Pc as rigid, i.e., neglecting the coupling between its intramolecular vibrations and the vdW vibrations of the adsorbed He atom, is not expected to introduce significant errors because of (a) the weak potential interaction between He and Pc and (b) the large disparity between the masses of He and Pc that minimizes the kinematic coupling. The intermolecular vibrations of M·R complexes are described in terms of the three Cartesian components (x, y, z) of the vector connecting the center of mass of M and the atom R. The Cartesian axes are aligned with the principal axes of M, with x and y in the direction of the two in-plane axes of the aromatic molecule, and z perpendicular to the molecular plane. These coordinates are suitable for describing the motions of an atom bound to a highly anisotropic nanosurface of the planar substrate. The vdW vibrational Hamiltonian in these M-fixed coordinates was derived by Brocks and van Koeven.[29]

The three intermolecular degrees of freedom of the M·R complexes are treated in the discrete variable representation (DVR).[30,31] The versatility and the efficiency of multidimensional DVRs have been demonstrated in demanding bound-state calculations arising in a wide range of problems, including most recently the translation-rotation dynamics of hydrogen molecules inside the cages of the clathrate hydrates[32,33] and C_{60}.[34,35] The multidimensional DVR can be tailored to the features of the PES and confined only to the physically relevant regions of

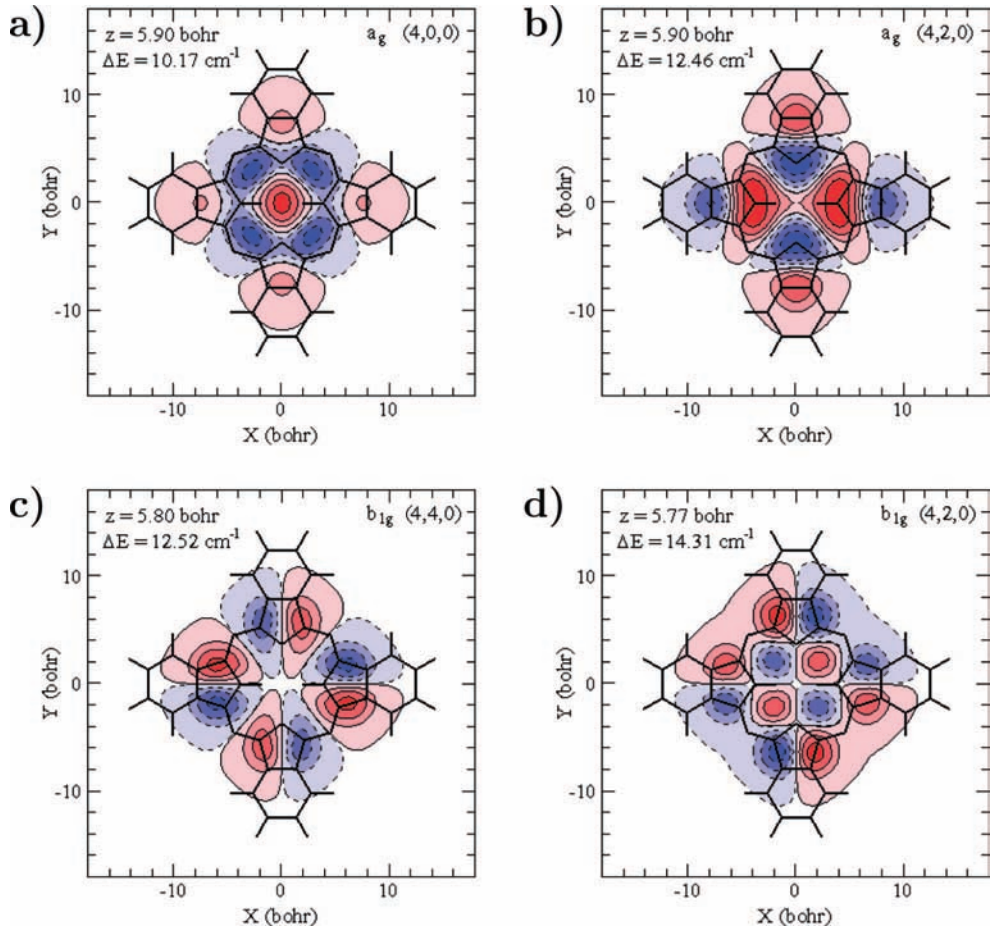

Figure 5. Cuts in the *xy* plane through the wave functions of four vdW vibrational states with four quanta in the in-plane modes at *z* corresponding to the expectation value $\langle z \rangle$ for each state. Contours are for 80%, 50%, 25%, and 1% of the maximum amplitude for the respective cuts.

the potential. Moreover, it permits an effective implementation of the sequential diagonalization and truncation procedure for reducing drastically the size of the final Hamiltonian matrix without loss of accuracy of the calculated eigenstates.[30,31,36]

The 3D DVR utilized in this work is constructed as a direct product of 1D DVRs defined by 1D harmonic oscillator (HO) functions in *x*, *y*, and *z*, respectively, with the origin in the center of mass of Pc. The feasible permutation-inversion (PI) symmetry group of Pc·He is D_{2h}, the same as for tetracene·He and pentacene·He.[20] As discussed at length previously,[24] the 3D DVRs symmetry adapted to the irreducible representations (IRs) of this group are formed as a direct product of 1D DVRs, one for each of the three Cartesian coordinates, which have the required parity, even or odd. The parities of the 1D DVRs in *x*, *y*, and *z* coordinates, respectively, needed to form the 3D DVRs transforming under the different IRs of the D_{2h} symmetry group are given in Table 1 of ref 24.

The very large amplitude of the vibrations of the He atom parallel to the molecular surface, including the possibility of the wave function delocalization over both sides of the substrate through side-crossing, mandates the use of the 3D DVR grid with a large spatial extent. The range of the DVR was from 0 to 19 au in the *x* and *y* coordinates, and from 0 to 15 au along the *z* coordinate. The dimensions of the 1D DVRs in *x*, *y*, and *z* directions were $N_x = N_y = 40$ and $N_z = 80$, respectively, resulting in a large direct-product 3D DVR basis, $N_x \times N_y \times N_z = 128\,000$. However, this basis was greatly reduced by means of the sequential diagonalization and truncation procedure. Thus, in the *z* coordinate, out of $N_z = 80$ 1D (*z* mode) eigenstates obtained for each pair of DVR points (x_α, y_β), only the $n_{cut}^{1D} = 30$ lowest energy 1D eigenstates were retained for the next step. For the last step, $n_{cut}^{2D} = 100$ lowest energy 2D (*yz*) eigenstates, out of $N_y \times n_{cut}^{1D} = 1200$, were kept at each DVR point x_α along the *x* axis. These basis set parameters were chosen after careful convergence tests. The dimension of the final Hamiltonian matrix, diagonalization of which yielded the 3D vdW vibrational eigenvalues and eigenvectors, was $N_x \times n_{cut}^{2D} = 4000$, far smaller than that of the original direct-product 3D DVR basis, 128 000.

B. Intermolecular Potential Energy Surface. As in our previous work on atom-large molecule vdW complexes, the IPES of Pc·He in the S_0 state was represented as a sum over pairwise 12−6 Lennard-Jones (LJ) potentials between the He atom and each atom of Pc, $C_{32}N_8H_{18}$. The LJ parameters employed in this work are shown in Table 1. They were used previously by Whitley et al.,[19] in their study of the microsolvation of Pc by helium clusters. The geometry of Pc was taken from the DFT calculation (B3LYP/6-31G*),[37] and is consistent with the experimental data obtained by neutron scattering.[38]

The Pc·He IPES constructed in this manner is shown in Figure 1. On either side of the molecular plane, there exist four equivalent global minima located within the five-membered rings, with the Cartesian coordinates (0.0, ±6.68, ±5.25 au) and (±6.80, 0.0, ±5.25 au), having the well depth $D_e = -138.1$ cm^{-1}. In addition, there are four equivalent local minima inside the central macrocycle between the five-membered rings, at (±2.38, ±2.67, ±5.49 au), with $D_e = -136.3$ cm^{-1}. Finally, two equivalent local minima exist near the center of Pc, on the *y* axis at (0.0, ±1.33, ±5.56 au), with $D_e = -130.5$ cm^{-1}.

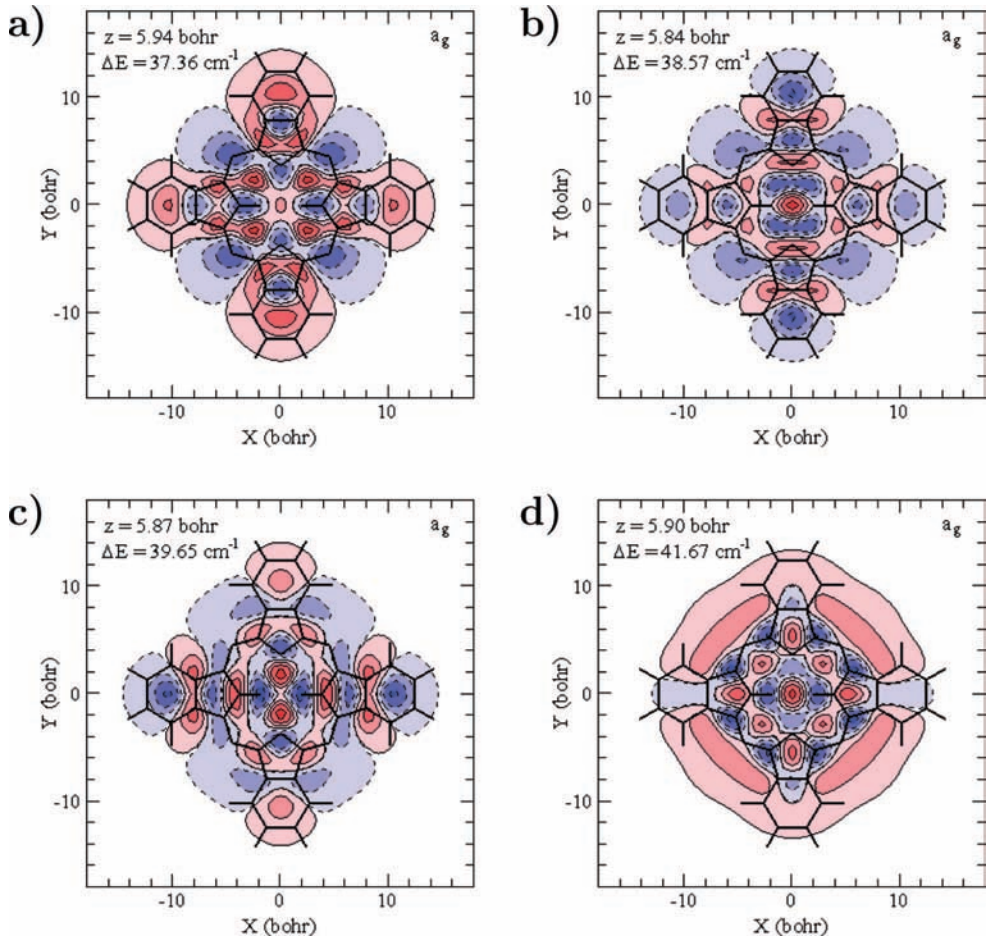

Figure 6. Cuts in the *xy* plane through the wave functions of four extensively delocalized vdW vibrational states with A_g symmetry at *z* corresponding to the expectation value $\langle z \rangle$ for each state. Contours are for 80%, 50%, 25%, and 1% of the maximum amplitude for the respective cuts.

III. Results and Discussion

The vdW vibrational levels of S_0 Pc·He calculated with the 3D DVR method are given in Table 2. They are labeled with two IRs of the D_{2h} symmetry group, since every level shown actually consists of a pair of nearly degenerate states which are symmetric and antisymmetric, respectively, with respect to the molecular plane. The root-mean-square (rms) amplitudes of the vdW vibrations, Δx, Δy, and Δz, along each of the Cartesian axes are also shown. They provide a measure of the floppiness of the complexes in each vibrational state, and are very useful for making the quantum number assignments. The expectation values of the Cartesian coordinates $\langle x \rangle$ and $\langle y \rangle$ are zero by symmetry. In principle, $\langle z \rangle = 0$ as well; however, in order to characterize the *z* location of the wave function relative to the molecular plane, we define $\langle z \rangle$ over the *positive z* range only, which is given in Table 2.

In Table 2, two distinct sets of quantum numbers are used to assign the in-plane (*xy*) vdW excitations. One set consists of the Cartesian quantum numbers $[v_x, v_y]$, denoting the number of quanta in the vibrational modes along the *x* and *y* axis, respectively. The second set is comprised of the quantum numbers (v, l) of the 2D isotropic oscillator, where *v* denotes the number of quanta and *l* is the vibrational angular momentum in the direction of the out-of-plane *z* axis; for a given *v*, *l* can take $v + 1$ values, $-v, -v + 2, \ldots, v - 4, v - 2, v$.[39] Which of these two sets of quantum numbers is appropriate for assigning a particular state is indicated by the appearance and symmetry of the nodal structure revealed by the *xy* cut through the wave function, as well as by the certain patterns present in the energy level structure. In the (v, l) quantization, the value of *l*, actually its absolute value $|l|$, can be determined by counting the number of angular nodes in the wave function perpendicular to the *xy* plane. In both cases, the *z*-mode excitations can be assigned the Cartesian quantum number v_z by counting the nodal planes perpendicular to the *z* axis, completing the quantum number assignment in terms of either $[v_x, v_y, v_z]$ or $(v, |l|, v_z)$. The quantum number assignments will be discussed in more detail shortly.

The vdW vibrational ground-state energy calculated for Pc·He is -92.27 cm^{-1}. Since the global minimum of the IPES is at -138.13 cm^{-1}, the ZPE of this vdW complex is 45.86 cm^{-1}, which represents ~33% of the potential well depth. To put this result in perspective, the ZPEs calculated in paper I[20] for S_1 tetracene·He and pentacene·He amount to ~39% of their respective well depths, -100.84 and -102.91 cm^{-1}.

A.. Excited van der Waals Vibrational States. The first two excited states in Table 2, [0, 1, 0] at 1.72 and [1, 0, 0] at 2.63 cm^{-1}, represent the *y*- and *x*-mode fundamentals, respectively. The slight difference in their frequencies is due to the two H atoms lying symmetrically on the *x* axis, close to the center of Pc, which have no counterparts on the *y* axis. Figure 2 shows that the amplitude of the state [0,1,0] has identical maxima at two (of the four) equivalent global minima inside the two five-membered rings on the *y* axis. The [1, 0, 0] wave function is identical with that of [0,1,0] apart from the rotation by 90°, so that its amplitude peaks at the other two equivalent global minima within the two five-membered rings on the *x*

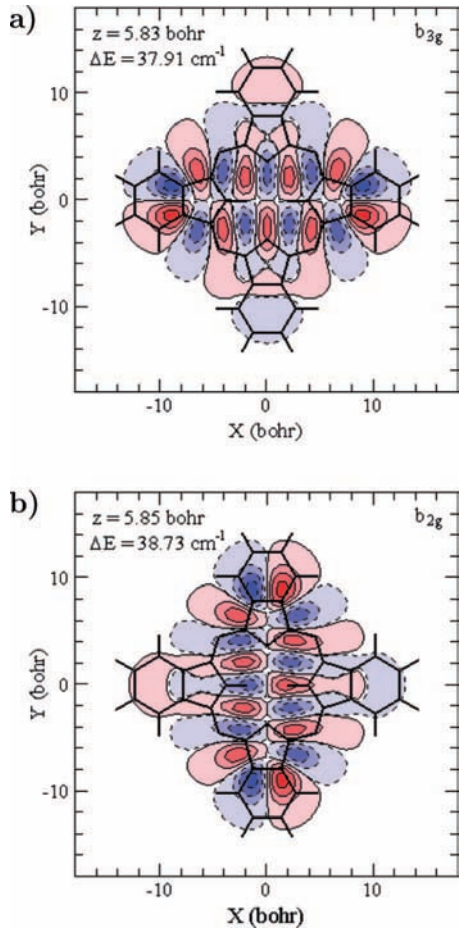

Figure 7. Cuts in the *xy* plane through the wave functions of the vdW vibrational states assigned as [8, 1, 0] (a) and [1, 8, 0] (b) at z corresponding to the expectation value $\langle z \rangle$ for each state. Contours are for 80%, 50%, 25%, and 1% of the maximum amplitude for the respective cuts.

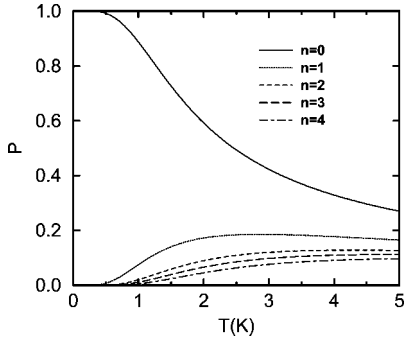

Figure 8. The populations of the ground ($n = 0$) and first four excited ($n = 1-4$) vdW vibrational states in Table 2 as a function of temperature.

TABLE 3: Spatial Delocalization of the Ground van der Waals Vibrational States of Phthalocyanine·He (S_0), Tetracene·He (S_1), and Pentacene·He (S_1)

complex	Δx (bohr)	Δy (bohr)	Δz (bohr)	$\langle z \rangle$ (bohr)
phthalocyanine·He	2.11	2.87	0.54	5.95
pentacene·He[a]	2.53	1.23	0.59	6.37
tetracene·He[a]	2.15	1.25	0.60	6.37

[a] Reference 20.

axis. In contrast, the ground-state wave function shown in Figure 2a has a maximum at the center of Pc.

The frequencies of the *x*- and *y*-mode fundamentals of Pc·He, both less than 3 cm^{-1}, are comparable to the fundamental frequency of the long-axis (x) mode of pentacene·He, 2.37 cm^{-1}, and considerably lower than that of its short-axis (y) mode, 11.26 cm^{-1} (Table 5 in paper I[20]). That the *x*- and *y*-mode fundamentals of Pc·He are much closer in frequency than those of pentacene·He is a reflection of the fact that the profiles of the IPES of the former complex along the x and y axes are much more similar with respect to the spatial extent and corrugation than those of the latter.

The next two higher states of Pc·He in Table 2 at 3.06 and 3.57 cm^{-1} have their wave functions displayed in Figure 3, panels a and b. It is evident that the quantum numbers (v, l) of the 2D isotropic oscillator, not the Cartesian quantum numbers, are appropriate for these two states, and that their assignments are (2, 2, 0) and (2, 0, 0), respectively. There should be three vdW states with $v = 2$, and indeed the third such state (2, 2, 0) is at 6.19 cm^{-1}, shown in Figure 3c. If these three in-plane excitations were harmonic, then their energies would depend on v only and not on l, i.e., they would be degenerate. Instead, the dependence on $|l|$ is quite pronounced, implying that the in-plane modes are anharmonic. We note that while the amplitudes of all three wave functions in Figure 3 have four identical maxima, for the two lower energy states the maxima are at (or very close to) the four equivalent global minima inside the five-membered rings, but for the highest energy state they appear at the four equivalent local minima between the five-membered rings.

The four states having three quanta of excitation in the in-plane modes, whose wave functions are shown in Figure 4, present an interesting case. These states are grouped into two pairs which are separated by about 7 cm^{-1}, while the members of each pair are less than 1 cm^{-1} apart. The two lower energy states at 4.97 and 5.65 cm^{-1} in panels a and b of Figure 4 can be assigned by using the Cartesian quantum numbers as [0, 3, 0] and, [3, 0, 0], respectively. But for the two higher energy states at 11.64 and 12.42 cm^{-1}, panels c and d of Figure 4 make it clear that the quantum numbers of the 2D isotropic oscillator should be used, and that assignment of both states is (3, 1, 0) (they belong to different IRs of the D_{2h} symmetry group).

We have encountered this type of alternating between [v_x, v_y, v_z] and (v, $|l|$, v_z) assignments in our earlier investigations of the intermolecular vibrations of the vdW complexes *o*-xylene·Ar[26] and 2,3-dimethylnaphthalene·He,[15] and of CO on the Cu(100) surface.[40] We believe that this happens because the wave functions associated with different eigenvalues sample regions of the IPES which differ subtly in their shape and mode couplings, giving rise to distinct nodal patterns and quantum numbers.[26]

Figure 5 shows the wave functions of four vdW states with four quanta in the in-plane modes. All four can be readily assigned in terms of the 2D isotropic oscillator quantum numbers, $v = 4$ and $l = 0$, 2, 4. Only one of the two $l = 4$ states could be positively identified, and its highly regular wave function is displayed in Figure 5c. The excitation energies of these four states range from 10.17 to 14.31 cm^{-1}, and their strong variation with $|l|$ provides additional evidence of the anharmonicity of the in-plane vibrations.

With increasing excitation energies, the nodal patterns of the wave functions grow in complexity, making the assignment more difficult and ambiguous. A typical example are the four states of A_g symmetry with their intricate wave functions shown in Figure 6, whose excitation energies span ~4 cm^{-1}, from 37.36 to 41.67 cm^{-1}. For this reason, many of the higher lying states

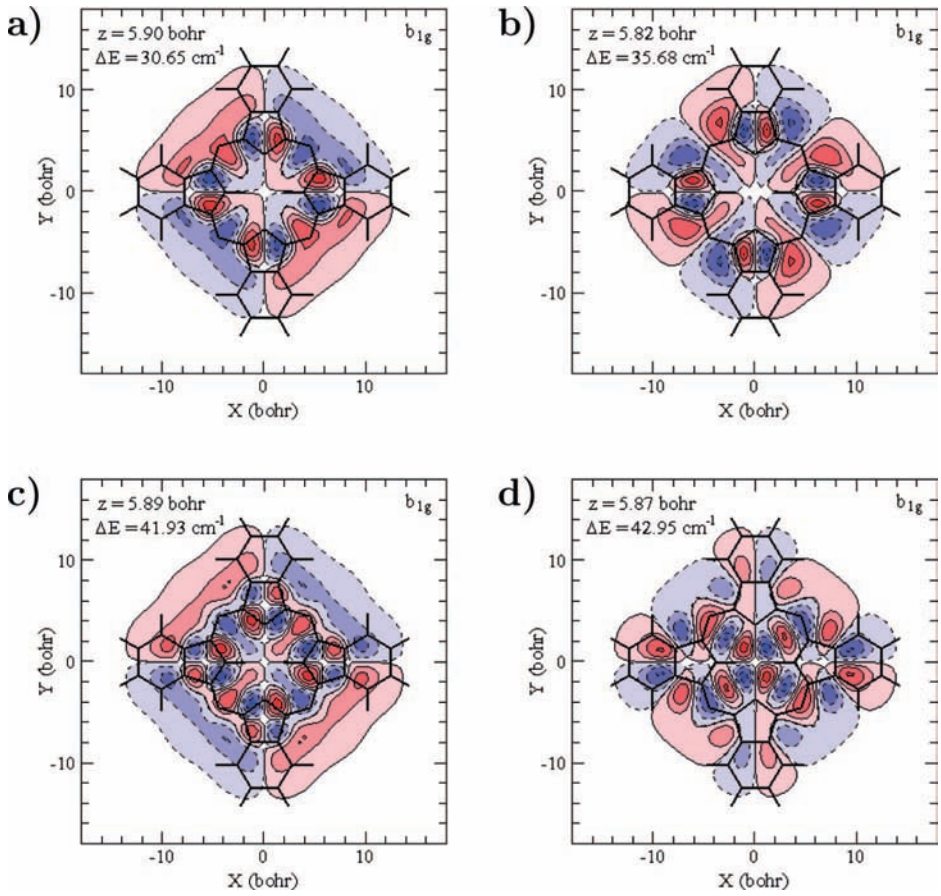

Figure 9. Cuts in the *xy* plane through the wave functions of four extensively delocalized vdW vibrational states with B_{1g} symmetry at *z* corresponding to the expectation value $\langle z \rangle$ for each state. Contours are for 80%, 50%, 25%, and 1% of the maximum amplitude for the respective cuts.

in Table 2 are left unassigned. The states lying in this energy range that we were able to assign have their excitations mainly along the *x* and *y* axes, with rather simple and regular nodal patterns, permitting assignment in terms of the Cartesian quantum numbers. Most of these assignable states belong to the progressions [v_x, 1, 0] and [1, v_y, 0], with v_x and v_y both ranging from 4 to 8. Two representative states [8, 1, 0] and [1, 8, 0] at 37.91 and 38.73 cm^{-1}, respectively, are shown in Figure 7. Interestingly, in both [v_x, 1, 0] and [1, v_y, 0] progressions for $v_x = 4-8$ and $v_y = 4-8$, the separation between the neighboring levels which differ by one quantum of excitation in either *x* or *y* is remarkably constant, 4.5−5.5 cm^{-1}. This is more than twice the frequencies of the *x*- and *y*-mode fundamentals, 2.63 and 1.72 cm^{-1}, respectively. On the other hand, this energy separation is consistent with that of ∼10 cm^{-1} between the pairs of Cartesian states [0, 3, 0] and [0, 5, 0] in Table 2, as well as [3, 0, 0] and [5, 0, 0], which differ by *two* quanta of excitation.

It is worth pointing out that for the states assigned with the Cartesian quantum numbers, such as those in Figures 2, 4a,b, and 7, the nodal planes of the wave functions are parallel to the diagonals of the square-shaped potential basin depicted in Figure 1a, rather than to its sides, and hence also to our chosen *x* and *y* axes. This is undoubtedly due to the topography of the IPES, whose four equivalent global minima lie on the diagonals of the square (see Figure 1a); in a sense, they anchor the wave function amplitudes which follow the square diagonals connecting the minima.

All the vdW vibrational states listed in Table 2 have $v_z = 0$. For tetracene·He and pentacene·He the fundamental excitation of the out-of-plane *z* mode was calculated in paper I[20] to lie at ∼38 cm^{-1}. However, in the case of Pc·He, although the states with energies up to about 45 cm^{-1} were carefully examined, none of them could be assigned as the *z*-mode fundamental. Two explanations are possible. One, which we consider less likely, is that the energy of the fundamental *z*-mode excitation is higher than 45 cm^{-1}, and thus remains to be identified. The alternative is that at the vdW excitation energies about 40 cm^{-1} and above, where the density of states is high (higher than for tetra- and pentacene·He), the coupling between the *z* mode and the in-plane excitations is very strong, resulting in highly mixed, irregular wave functions. In this case an eigenstate with pure or predominantly *z*-mode excitation simply does not exist.

Finally, Figure 8 shows the populations of the ground and the first four excited vdW vibrational states in Table 2, in the temperature range 0−5 K. At the temperature of the He droplets, 0.38 K, Pc·He is exclusively in the ground vdW state, despite the low frequencies of the *x*- and *y*-mode fundamentals. The lowest excited states begin to be appreciably populated above 1 K.

B. Spatial Delocalization of the He Atom on the Aromatic Nanosurface. The issue of the extent of spatial delocalization of the He atom on planar aromatic nanosurfaces has received considerable attention. Table 3 shows the rms amplitudes Δx, Δy, and Δz for the ground vdW vibrational state of Pc·He computed in his work, together with those for tetra- and pentacene·He reported in paper I.[20] Judging from Δx and Δy values, 2.11 and 2.87 au, the wave function delocalization parallel to the Pc surface is large already in the ground state, and similar in both *x* and *y* directions, as expected for a square-shaped substrate. This spatial delocalization is comparable to that of tetracene·He and pentacene·He in the direction of the long (*x*) axis, with Δx of 2.15 and 2.53 au, respectively.

However, for these two vdW complexes, the delocalization along the other in-plane axis (y) is about a factor of 2 smaller, Δy being equal to 1.25 and 1.23 au, respectively. The rms amplitude Δz in the ground state, 0.5−0.6 au, is similar for all three complexes. Its value, which is 4−5 times smaller than Δx (as well as Δy for Pc), indicates that the motion of the He atom perpendicular to the molecular plane is considerably more constrained than in the directions parallel to it. The vibrationally averaged distance $\langle z \rangle$ of the He atom to the aromatic plane varies little among the three complexes, from 6.0 to 6.4 au.

Excitation of the in-plane vdW vibrational modes causes rapidly increasing wave function delocalization parallel to the nanosurface of Pc. Thus, for the progression of states [υ_x, 1, 0] Δx grows from 4.88 au for $\upsilon_x = 4$ to 6.84 au for $\upsilon_x = 8$. Likewise, for the [1, υ_y, 0] progression, Δy increases from 4.40 au for $\upsilon_y = 4$ to 6.93 au for $\upsilon_y = 8$. In fact, $\Delta x = 6.84$ au for the state [8, 1, 0] and $\Delta y = 6.93$ au for the state [1, 8, 0], both shown in Figure 7, represent the largest rms amplitudes in x and y, respectively, for the excitation energies up to ∼43 cm^{-1}. Many other excited states are delocalized fairly uniformly in all in-plane directions, and have Δx and Δy values which are nearly equal. Four such high-lying states of B_{1g} symmetry with excitation energies up to 43 cm^{-1} are displayed in Figure 9. Their wave functions are strikingly square-shaped, and are bounded by the (square) potential contour in Figure 1a drawn at −49 cm^{-1} (43.3 cm^{-1} above the ground state). These wave functions are spread over the entire nanosurface of Pc accessible at these excitation energies. In contrast, for all the states considered Δz is about 0.6 au, which is an order of magnitude smaller than the largest Δx and Δy values. Clearly, the physisorbed He atom moves much more freely parallel to the nanosurface than perpendicular to it.

For the states of Pc·He analyzed in this work, with excitation energies up to about 45 cm^{-1}, the He atom is completely confined to one side of the molecular plane. This is evident from the cuts through the wave functions in the xz and yz planes, which show no appreciable amplitude around the aromatic molecule, close to the $z = 0$ plane. Additional evidence is provided by the lack of energy splitting of the pairs of states in Table 2 which are symmetric/antisymmetric with respect to the molecular plane. In this energy range, any tunneling splitting that may be present is smaller than 0.001 cm^{-1}. The reason for the confinement is apparent from Figure 1b, where the yz cut through the IPES for $x = 0.0$ au is shown (the xz cut is virtually identical). The contour at −49 cm^{-1}, corresponding to the excitation energy of 43 cm^{-1}, is entirely localized on one side of the molecular plane. The crossing of the He atom from one side to the other becomes possible only at considerably higher energies, as shown by the contour drawn at −13 cm^{-1}, which encloses both sides of the molecule.

In this respect, Pc·He differs considerably from tetracene·He and pentacene·He analyzed in paper I.[20] Starting at about 30 cm^{-1}, the vdW vibrational states of both these complexes exhibit tunneling splittings greater than 0.001 cm^{-1}, which increase to 0.08 cm^{-1} or more at ∼40 cm^{-1}. The larger tunneling splittings are associated with significant excitation of the y mode, in the direction of the short (y) molecular axis, because it offers a shorter side-crossing path, and because the moment of inertia of the aromatic molecule for the side-crossing motion of He is smaller in the y than in the x direction.[15,20] In the case of Pc·He, there is no short molecular axis; the x and y axes are essentially equivalent, and both side-crossing paths are equally long.

IV. Conclusions

We have reported a rigorous quantum mechanical study of the large-amplitude intermolecular vibrations of the van der Waals (vdW) complex phthalocyanine·He (Pc·He) in the ground electronic state S_0. This study contributes to our quantitative understanding of the excited vdW vibrations of the He atom physisorbed on the corrugated nanosurfaces of large planar aromatic molecules. It complements our recent investigations of the quantum dynamics of the vdW vibrational eigenstates of weakly bound complexes tetracene·He and pentacene·He in the S_1 state.[20] The Pc molecule has a square shape, unlike tetracene and pentacene which are essentially rectangular, with one in-plane molecular axis considerably longer than the other. The energy level structure and the quantum number assignments of the vibrational excitations of the He atom parallel to the nanosurface of Pc, which is square-shaped and with a distinct corrugation pattern, differ qualitatively from those calculated previously[20] for tetra- and pentacene·He.

The vdW vibrational eigenstates of Pc·He were calculated accurately, as fully coupled, while the Pc molecule was treated as rigid. The 3D DVR bound-state method[24] was utilized, yielding eigenvalues and eigenfunctions of the 3D intermolecular vibrational Hamiltonian[29] which are numerically exact for the IPES employed. The IPES of Pc·He was represented as a sum of atom−atom Lennard-Jones pair potentials, with the parameters taken from a theoretical study of Pc in helium clusters.[19] The four equivalent global minima of this IPES with the well depth of −138 cm^{-1} are each located inside one of the five-membered rings near the corners, and on the diagonals, of the square substrate. For comparison, the IPESs of tetra- and pentacene·He have their global and local minima lined up along the longer of the two in-plane molecular axes.[20] The unique topography of the IPES of Pc·He leaves a clear imprint on the excited vdW vibrational wave functions.

The excited vdW vibrational states of Pc·He analyzed in this paper reach up to about two-thirds of the well depth of the IPES. The fundamental excitations along the two molecular axes (x and y) parallel to the substrate surface have low frequencies of 2.63 and 1.72 cm^{-1}, respectively. The assignment of the in-plane vdW vibrational excitations requires the use of both the Cartesian quantum numbers [υ_x, υ_y] and the quantum numbers (υ, l) of the 2D isotropic oscillator, depending on the symmetry and the nodal patterns of the wave functions. The Cartesian quantum number υ_z for the out-of-plane z mode completes the assignment of the 3D eigenstates as either [υ_x, υ_y, υ_z] or (υ, $|l|$, υ_z). As the excitation energy increases, the nodal patterns of the wave functions become much more complex and the ambiguity about the assignments grows. At higher excitation energies, two progressions of assignable states stand out, [υ_x, 1, 0] and [1, υ_y, 0], with υ_x and υ_y taking values from 4 to 8. Their wave function amplitudes are predominantly localized along the diagonals of the square-shaped nanosurface of Pc. In both progressions, the neighboring levels are evenly separated by 4.5−5.5 cm^{-1}. In the range of excitation energies considered, up to 45 cm^{-1}, no eigenstate could be identified with any confidence as the z-mode fundamental, presumably as a result of the strong coupling in this energy range between the vdW excitations perpendicular and parallel to the molecular plane.

The He atom is extensively delocalized along the surface of Pc already in the ground vdW state, with the rms amplitudes Δx and Δy equal to 2.11 and 2.87 au, respectively. The degree of delocalization parallel to the molecular surface increases rapidly with the excitation of the in-plane vdW vibrations, reaching maximum Δx and Δy values of 7 au at energies around

40 cm^{-1}. Many of the highly excites states are delocalized over the entire available nanosurface; their wave functions in the *xy* plane are remarkably square-shaped, reflecting the shape of the substrate. The vdW vibrational wave functions are an order of magnitude more localized perpendicular to the Pc surface, with Δz of about 0.6 au for all the eigenstates examined. For the excitation energies probed in this study, the He atom is completely confined to one side of the molecular plane.

A higher quality IPES for the He−Pc interaction is needed, and so are additional spectroscopic data regarding the vdW vibrational excitations of the Pc·He dimer. We are developing a rigorous computational approach for calculating the excited vdW eigentates of two or more He atoms bound to the nanosurface of a large molecule. It builds on our DVR/sequential diagonalization and truncation scheme for a single adsorbed rare-gas atom[24] and incorporates some other recent developments in the methodology for high-dimensional bound state calculations.[41]

Acknowledgment. Z.B. is grateful to the National Science Foundation for partial support of this research, through Grant CHE-0315508. The computational resources used in this work were funded in part by the NSF MRI grant CHE-0420870. Acknowledgment is made to the donors of the American Chemical Society Petroleum Research Fund for partial support of this research.

References and Notes

(1) Toennies, J. P.; Vilesov, A. F. *Annu. Rev. Phys. Chem.* **1998**, *49*, 1.
(2) Callegari, C.; Lehmann, K. K.; Schmied, R.; Scoles, G. *J. Chem. Phys.* **2001**, *115*, 10090.
(3) Stienkemeier, F.; Vilesov, A. F. *J. Chem. Phys.* **2001**, *115*, 10119.
(4) Hartmann, M.; Lindinger, A.; Toennies, J. P.; Vilesov, A. F. *Chem. Phys.* **1998**, *239*, 139.
(5) Hartmann, M.; Lindinger, A.; Toennies, J. P.; Vilesov, A. F. *J. Phys. Chem. A* **2001**, *105*, 6369.
(6) Hartmann, M.; Lindinger, A.; Toennies, J. P.; Vilesov, A. F. *Phys. Chem. Chem. Phys.* **2002**, *4*, 4839.
(7) Lehnig, R.; Slenczka, A. *J. Chem. Phys.* **2003**, *118*, 8256.
(8) Lehnig, R.; Slenczka, A. *J. Chem. Phys.* **2004**, *120*, 5064.
(9) Lehnig, R.; Slenczka, A. *ChemPhysChem* **2004**, *5*, 1014.
(10) Lindinger, A.; Toennies, J. P.; Vilesov, A. F. *J. Chem. Phys.* **2004**, *121*, 12282.
(11) Lehnig, R.; Slipchenko, M.; Kuma, S.; Momose, T.; Sartakov, B.; Vilesov, A. F. *J. Chem. Phys.* **2004**, *121*, 9396.
(12) Krasnokutski, S.; Rouillé, G.; Huisken, F. *Chem. Phys. Lett.* **2005**, *406*, 386.
(13) Lehnig, R.; Slenczka, A. *J. Chem. Phys.* **2005**, *122*, 244317.
(14) Lehnig, R.; Sebree, J. A.; Slenczka, A. *J. Phys. Chem. A* **2007**, *111*, 7576.
(15) Bačić, A.; Leutwyler, S.; Sabo, D.; Bačić, Z. *J. Chem. Phys.* **1997**, *107*, 8781.
(16) Even, U.; Al-Hroub, I.; Jortner, J. *J. Chem. Phys.* **2001**, *115*, 2069.
(17) Even, U.; Jortner, J.; Noy, D.; Lavie, N.; Cossartagos, C. *J. Chem. Phys.* **2000**, *112*, 8068.
(18) Huang, P.; Whitley, H. D.; Whaley, K. B. *J. Low Temp. Phys.* **2004**, *134*, 263.
(19) Whitley, H. D.; Huang, P.; Kwon, Y.; Whaley, K. B. *J. Chem. Phys.* **2005**, *123*, 054307.
(20) Xu, M.; Bačić, Z. *J. Phys. Chem. A* **2007**, *111*, 7653.
(21) Heidenreich, A.; Even, U.; Jortner, J. *J. Chem. Phys.* **2001**, *115*, 10175.
(22) Heidenreich, A.; Jortner, J. *J. Chem. Phys.* **2003**, *118*, 10101.
(23) Felker, P. M.; Neuhauser, D. *J. Chem. Phys.* **2003**, *119*, 5558.
(24) Mandziuk, M.; Bačić, Z. *J. Chem. Phys.* **1993**, *98*, 7165.
(25) Mandziuk, M.; Bačić, Z.; Droz, T.; Leutwyler, S. *J. Chem. Phys.* **1994**, *100*, 52.
(26) Droz, T.; Leutwyler, S.; Mandziuk, M.; Bačić, Z. *J. Chem. Phys.* **1994**, *101*, 6412.
(27) Droz, T.; Leutwyler, S.; Mandziuk, M.; Bačić, Z. *J. Chem. Phys.* **1995**, *102*, 4715.
(28) Droz, T.; Leutwyler, S.; Mandziuk, M.; Bačić, Z. *J. Chem. Phys.* **1995**, *103*, 4855.
(29) Brocks, G.; van Koeven, D. *Mol. Phys.* **1988**, *63*, 999.
(30) Bačić, Z.; Light, J. C. *Annu. Rev. Phys. Chem.* **1989**, *40*, 469.
(31) Bačić Z. Bound states of strongly coupled multidimensional molecular Hamiltonians by the discrete variable representation approach. In *Domain-Based Parallelism and Problem Decomposition Methods in Computational Science and Engineering*; Keyes, D. E., Saad Y., Truhlar, D. E., Eds.; SIAM: Philadelphia, PA, 1995; p 263.
(32) Xu, M.; Elmatad, Y.; Sebastianelli, F.; Moskowitz, J. W.; Bačić, Z. *J. Phys. Chem. B* **2006**, *110*, 24806.
(33) Xu, M.; Sebastianelli, F.; Bačić, Z. *J. Chem. Phys.* **2008**, *128*, 244715.
(34) Xu, M.; Sebastianelli, F.; Bačić, Z.; Lawler, R.; Turro, N. J. *J. Chem. Phys.* **2008**, *128*, 011101.
(35) Xu, M.; Sebastianelli, F.; Bačić, Z.; Lawler, R.; Turro, N. J. *J. Chem. Phys.* **2008**, *129*, 064313.
(36) Bačić, Z.; Light, J. C. *J. Chem. Phys.* **1987**, *86*, 3065.
(37) Gong, X. D.; Xiao, H. M.; Tian, H. *Int. J. Quantum Chem.* **2002**, *86*, 531.
(38) Hoskins, B. F.; Mason, S. A.; White, J. C. B. *J. Chem. Soc. D* **1969**, *10*, 554.
(39) Landau, L. D.; Lifshitz, E. M. *Quantum Mechanics*; Pergamon Press: Oxford, UK, 1977.
(40) Bahel, A.; Bačić, Z. *J. Chem. Phys.* **1999**, *111*, 11164.
(41) Bowman, J. M.; Carrington, T.; Meyer, H. D. *Mol. Phys.* **2008**, *106*, 2145.

JP809410S